Article

Discovery Medicine 2023; 35(178): 831–844
https://doi.org/10.24976/Discov.Med.202335178.78

Therapeutic Effect of Human Bone Marrow- and Adipose-Derived Stem Cells on Intervertebral Disc Degeneration: A Comparative Study on Rats

Jin Zhang[1,†], Jie Pan[2,†], Gonghua Dai[2], Xuesong Li[3], Zhongmin Zhang[3], Lijun Li[2,*], Bin Shen[2,*]

[1]Department of Spinal Surgery, Shanghai East Hospital, Tianjin Medical University, 200120 Shanghai, China
[2]Department of Spinal Surgery, Shanghai East Hospital, Tongji University School of Medicine, 200120 Shanghai, China
[3]Clinical Medicine, Tianjin Medical University, 301700 Tianjin, China
*Correspondence: liliju@163.com (Lijun Li); sanly621@163.com (Bin Shen)
[†]These authors contributed equally.
Published: 1 October 2023

Background: Intervertebral disc degeneration (IVD) is a pain-inflicting disorder, posing a serious threat to the elderly, and new therapies are urgently needed. In this study, we examined the potential therapeutic effect of mesenchymal stem cells (MSCs) transplantation on IVD.

Methods: Both human adipose-derived stem cells (hADSCs) and human bone marrow mesenchymal stem cells (hBMSCs) provided by a volunteer were non-contact co-cultured with the human nucleus pulposus cells (hNPCs) to determine the efficacy of hNPCs-oriented differentiation. Flow cytometry was used to characterize the purity of hADSCs/hBMSCs. We determined the expression of surface antigen molecules, such as CD73, CD105, CD90, CD31, HLA-DR, CD34 and CD45, using flow cytometry. Osteogenic and lipogenic differentiations demonstrated by the cells were identified with Alizarin red and Oil red O staining, respectively, and changes in type II collagen and proteoglycan levels were detected by immunofluorescence. Myeloid cell-related mRNA and protein expression levels were detected by quantitative real-time polymerase chain reaction (qRT-PCR) and Western blot, respectively. The therapeutic effect of hADSCs and hBMSCs on IVD was evaluated in experimental rats, in which degeneration was induced by needling the annulus fibrosus of the caudal intervertebral disc.

Results: As evidenced by the presence of hNPCs-like morphology, both hBMSCs and hADSC could effectively differentiate into hNPCs. Using flow cytometry assays, we found high expression of type II collagen (COL2) and aggrecan (ACAN) protein in the hNPCs-like tissue. Treatment with hADSCs and hBMSCs attenuated IVD progression in the rats, and most importantly, there was no significant difference between the therapeutic effects of both types of cells on IVD, on the basis of the COL2 and SRY-Box Transcription Factor 9 (SOX9) protein expression and the histological results. Findings from the animal studies also suggested that both hADSCs and hBMSCs transplantation could be applied in IVD treatment.

Conclusions: In summary, both hADSCs and hBMSCs can attenuate the progression of IVD by delaying, rather than completely reversing the deterioration of disc degeneration, and there is no significant difference between hADSCs and hBMSCs on the therapeutic effects.

Keywords: intervertebral disc degenerative; human bone marrow mesenchymal stem cells; human adipose-derived stem cells; human nucleus pulposus cells

Introduction

Intervertebral disc degeneration (IVD) is a common condition in the elderly and is the main cause of neck, middle back and lower back pain [1]. Operation on IVD accounts for 80% of all elective surgeries on the spine, and relevant medical expenses exceed $30 billion each year [2]. Intervertebral discs are fibrocartilaginous structures inserted between adjacent vertebral bodies in the spine, and each disc is made up of chondrocytic endplates, a nucleus pulposus (NP), and an annulus fibrosus that surround the NP. Functionally, intervertebral discs allow the movement of the spine while transmitting force from one vertebra to another, and this function is mainly executed owing to the ability of NP to attract and retain water and thus hold the compressive loads. Intervertebral discs undergoing degeneration are characterized by changes in volume, structure, shape, and composition, as well as the reduction in the number of chondrocytes and the amount of type II collagen and proteoglycan in the extracellular matrix (ECM). These changes consequently decrease the mechanical function of the intervertebral disc and thus its ability to hold

compressive loads. In the past few decades, the molecular mechanisms underlying IVD progression have been extensively studied, and several key factors, such as SRY-Box Transcription Factor 9 (SOX9), transforming growth factor beta 1 (TGF-β1), TIMP metallopeptidase inhibitor 1 (TIMP1), bone morphogenetic protein 2 (BMP2), bone morphogenetic protein 7 (OP1), and latent membrane protein 1 (LMP1), were identified [3–5]. Furthermore, transfecting adenovirus strains expressing these genes into NP cells improved collagen and proteoglycan levels and restored ECM or cellular components to a certain degree in animal models [6–8], but this method does not increase the number of NP cells, limiting this method as a potential treatment approach for IVD.

In several animal models, autologous NP cell transplantation has shown good results in IVD treatment. However, it is challenging to widely adopt this method in clinical settings, given the fact that it is extremely difficult to gather a sufficient amount of NP cells required for this method and the collection of NP cells poses a damaging impact on the intervertebral discs of the donor where these cells were retrieved from. To address this conundrum, mesenchymal stem cells (MSCs) have recently become an attractive option as a viable alternative source of cells applied in cell transplant treatment due to their multilineage differentiating capacity [9,10]. MSCs can be divided into several groups according to their origin; some examples include bone marrow-derived MSCs (BMSCs), adipose-derived MSCs (ADSCs), and umbilical cord MSCs. These cells possess a special capacity for differentiation into a variety of cell types, such as osteoblasts, adipocytes, chondrocytes, and myocytes, making them ideal for cell-based IVD therapy [2]. In the present study, we investigated the therapeutic effect of stem cells on disc degeneration, both *in vitro* and *in vivo*.

Materials and Methods

Cell Source

In this study, the human bone marrow mesenchymal stem cells (hBMSCs), human adipose-derived stem cells (hADSCs), and human nucleus pulposus cells (hNPCs) were obtained from a 37-year-old male patient with intervertebral disc herniation, who was treated in Shanghai East Hospital. A routine examination was performed to find out other diseases, including infectious diseases and tumors. The patient and his family members consented to donate the cells after having been informed of the study objectives. The acquired cells were subjected to short tandem repeat (STR) profiling, and the present study only applied cells that are free from mycoplasma contamination.

Animal Source

We purchased 15 healthy male Sprague-Dawley (SD) rats from Nanjing University's Animal Center. The rats were 8 weeks old and weighed 250 g each. In order to ensure normal performance before the experiment, three animals per cage were reared with free access to food and water.

Extraction and Cultivation of Human Bone Marrow Mesenchymal Stem Cells

The collection of hBMSCs involves exposing the contralateral vertebral arch. A hard puncture sleeve with a 4-mm diameter was used to puncture through the vertebral arch and into the vertebral body along the standard puncture path. A syringe was connected to the back of the sleeve to collect approximately 20 mL of bone marrow under negative pressure. Heparin sodium (12,500 U), equivalent to half a dose of anticoagulant, was added to the collected bone marrow. The collection process followed a strict aseptic operation procedure. Once all specimens were collected, they were transported to the laboratory for further processing in a low-temperature transport box, which kept the tissue temperature between 4 and 6 °C. The transport time should be less than 30 minutes. hBMSCs were obtained using techniques that have been described elsewhere [11,12]. A 10 mL syringe preloaded with mesenchymal stem cell medium (MSCM; ScienCell, Carlsbad, CA, USA; Cat#7501), 5% fetal bovine serum (FBS; ScienCell, Carlsbad, CA, USA; Cat#0025), and mesenchymal stem cell growth supplement (MSCGS; ScienCell, Carlsbad, CA, USA; Cat#7552) was used to flush the complete bone marrow freshly collected from the patient. After incubating the cells at 37 °C in a humid environment containing 5% CO_2 for 48 hours, the medium was changed, eliminating the non-adherent cells. The cells were divided, replated, and passaged once they had achieved 80% confluency. Following that, induced differentiation and transplant operations were performed using BMSCs.

Extraction and Cultivation of Human Adipose-Derived Stem Cells

To collect hADSCs, an area containing subcutaneous adipose tissue was surgically incised using surgical scissors. Electrocautery should be avoided to prevent damage to the adipose tissue. Two pieces of adipose tissue, each with a size of approximately 3 cm by 3 cm, were excised. The collected tissues were then placed in a sterile specimen jar containing physiological saline. The collection process followed a strict aseptic operation procedure. Once all specimens were collected, they were transported to the laboratory for further processing in a low-temperature transport box, which kept the tissue temperature between 4 and 6 °C. The transport time should be less than 30 minutes. The adipose tissues were briefly washed with saline soon after extraction. After physically removing tiny vessels from the extracted tissues, the adipose tissues were then digested with 0.15% (w/v) collagenase I (Sigma, St. Louis, MO, USA) at 37 °C for 40 minutes. After digestion, the suspension was run through a 70-µm nylon mesh fil-

Table 1. Modified Thompson grading criteria.

Grade	T2W1 signal intensity and area changes
Grade 1	Normal signal intensity
Grade 2	Minimum decrease of signal intensity without obvious narrowing of high signal area
Grade 3	Moderate decrease in signal intensity
Grade 4	The maximum decrease in signal intensity

T2WI, T2 weighted image.

Table 2. Histomorphometric scoring criteria for intervertebral discs.

	Morphological changes of the intervertebral disc under light microscopy	Score
I – Fiber ring	The normal texture of the fibrocartilage layer without rupture or distortion	1
	Less than 30% of the fiber rings are broken and twisted	2
	Broken and twisted fibers exceeding 30% of the fiber ring	3
II – Boundary between the fibrous ring and the NP	Normal	1
	Micro interruptions	2
	Moderate or severe interruptions	3
III – Cells in the NP	Normal cells in a gel-like matrix contain a large number of vacuoles	1
	The slight reduction in the number of cells and vacuoles	2
	Moderately or severely reduced cell numbers; no vacuoles	3
IV – Stroma in the NP	Normal gel-like appearance	1
	Micro-condensation in the matrix	2
	Moderate or severe coagulation of the substrate	3

NP, nucleus pulposus.

ter to remove any remaining tissue debris. The suspension was centrifuged at 1300 rpm for 5 minutes, and the supernatant was discarded. The stromal cell pellet was suspended in MSCM (ScienCell, Carlsbad, CA, USA, Cat#7501) that comprised 100 U/mL penicillin/streptomycin solution, 2 µM GlutaMAX™ (Gibco, Waltham, MA, USA, Cat#35050061), 10 ng/mL epidermal growth factor (Sigma, St. Louis, MO, USA), 5% FBS (ScienCell, Carlsbad, CA, USA, Cat#0025), and MSCGS (No.#7501, ScienCell, Carlsbad, CA, USA). These cells were treated with 1 mL of 0.25% trypsin/ethylenediaminetetraacetate acid (EDTA) for 3 minutes after being rinsed with 0.01 M phosphate-buffered saline (PBS) after they had achieved 80% confluency. The cells were divided, replated, and passaged each time they reached 80% confluency.

Extraction and Cultivation of Human Nucleus Pulposus Cells

Additionally, the patient's hNPCs were further isolated to induce NPCs-oriented differentiation from hBMSCs and hADSCs. The collected NP was rinsed on an ultra-clean table with PBS, and the excess tissue was trimmed. Dulbecco's Modified Eagle Medium/Nutrient Mixture F-12 (DMEM/F12) without FBS was added to the NP. Following centrifugation at 1500 rpm for 5 minutes, the supernatant was discarded. Afterward, the NP was digested with 10 mL of 0.2% type II collagenase for 4 hours at 37 °C. The suspension was then centrifuged at 1500 rpm for 5 minutes, and the supernatant was discarded. Five milliliters of DMEM/F12 containing 15% FBS was added, and the cells were resuspended at a density of 1×10^5 cells/mL in a culture flask. The cells were incubated at 37 °C, 5% CO_2, for 3 days. The culture medium was changed every 7 days with 5 mL of DMEM/F12 containing 15% FBS, and the cells were passaged when they reached about 80% confluency. After hNPCs were inoculated and cultured for 24 hours, a small amount of adherent elliptical cells was observed; 72 hours later, the number of spindle-shaped or polygonal cells increased and a dramatic increase in cell number was observed at day 6–7. Meanwhile, most of the cells appeared as long-spindle or polygonal. When the cell reached 80% confluency, trypsinization and passaging were carried out.

Mesenchymal Stem Cell Assessment Using Flow Cytometry

hADSCs and hBMSCs were isolated using 0.25% trypsin plus 0.02% EDTA. The 50 mL cell suspension with a concentration of 10^6 cells/mL, after being cleaned with 0.01 M PBS, was used as the test set. Assay blocks were incubated with CD90 antibody (BD Pharmingen™, San Diego, CA, USA; Cat#551401), CD44 antibody (BD Pharmingen™, San Diego, CA, USA; Cat#550974), CD45 antibody (BD Pharmingen™, San Diego, CA, USA; Cat#559135), or CD29 antibody (BD Pharmingen™, San Diego, CA, USA; Cat#555005). The cells were directly examined with a flow cytometer (BD FACSCalibur; Becton Dickinson, Franklin Lakes, NJ, USA) following a 20-minute incubation in complete darkness at ambient temper-

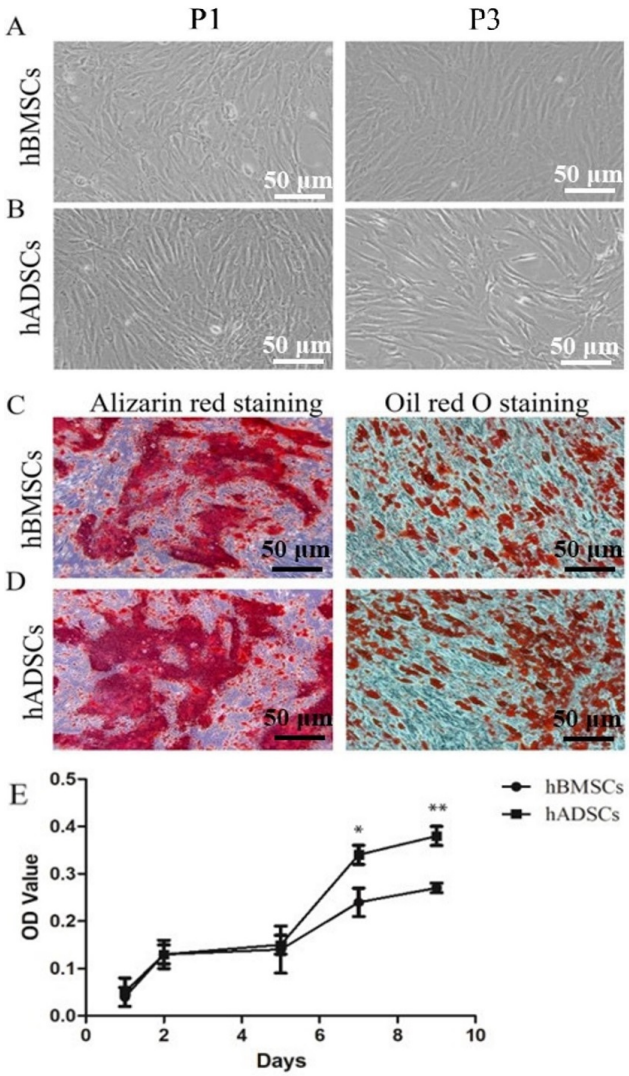

Fig. 1. Morphology and differentiation capacity of human bone marrow mesenchymal stem cells (hBMSCs) and human adipose-derived stem cells (hADSCs). (A) The morphology of hBMSCs was observed under 10× magnification. (B) The morphology of hADSCs was observed under 10× magnification. P1, first generation; P3, third generation. (C) Adipogenic or osteogenic induction medium was used for three weeks to induce the differentiation of hBMSCs after being stained with Alizarin red or Oil red O respectively; under 20× magnification. (D) Adipogenic or osteogenic induction medium was used for three weeks to induce the differentiation of hADSCs after being stained with Alizarin red or Oil red O respectively; under 20× magnification. (E) Cell Counting Kit-8 (CCK8) assay was performed to determine the proliferation of hBMSCs and hADSCs (n = 5, respectively). *$p < 0.05$, **$p < 0.01$, compared with each other.

ature. For data collection and processing, Becton Dickinson's Lysis II software (Nippon Becton Dickinson, Tokyo, Japan) was employed.

Co-Culture of MSCs and hNPCs

The co-culture device, which was designed to juxtapose the hBMSCs/hADSCs and hNPCs as reported earlier, was composed of a six-well plate placed at the bottom as well as a Transwell cell culture insert placed on the top (with a pore size of 0.4 m; BD Falcon, Nantong, China; Cat#353090) [13]. In brief, hADSCs were grown on the Transwell cell culture insert at a density of 2×10^5 cells per 9.6 cm^2, whereas hBMSCs were cultured in the six-well plate at a density of 1×10^5 cells per 9.6 cm^2. The co-culture media used was MSCM (ScienCell, Carlsbad, CA, USA; Cat#7501) with 15% FBS (ScienCell, Carlsbad, CA, USA; Cat#0025), 100 U/mL penicillin/streptomycin solution, as well as MSCGS (ScienCell, Carlsbad, CA, USA; Cat#7552). In a similar setup, isolated hNPCs, hADSCs, and hBMSCs were plated without any cells in the Transwell cell culture insert placed on top. Both co-culture and control culture lasted for 7 days.

Cell Viability Assay

The Cell Counting Kit-8 (CCK8; Beyotime Institute of Biotechnology, Nantong, China) was used to measure cell viability. In 96-well microplates, hBMSCs and hADSCs were grown at a concentration of 5000 cells per well. When these cells reached 80% confluency, they were passaged. On days 1, 2, 5, 7 and 9, these cells were subjected to CCK8 assay following the instruction of the manufacturer, and absorbance value was read at the wavelength of 450 nm using a 96-well plate reader (BioTek, Winooski, VT, USA), and the absorbance values were inversely correlated with cell survival.

Transplantation of Human Mesenchymal Stem Cells in IVD Treatment

According to the literature [14], the animal model of IVD was established. 15 rats, each using 6 discs, for a total of 90 discs, were divided into four groups: Group A was the hADSCs transplantation group (Group A, hADSCs-1, hADSCs-2), which consisted of two consecutive punctured degenerated discs, and hADSCs were applied as seed cells for disc repair within the degenerated discs. Group B was the hBMSCs transplantation group (Group B, hBMSCs-1, hBMSCs-2), which contained two consecutive punctured degenerated discs, and hBMSCs were applied as seed cells for disc repair within the degenerated discs. Group C was the degeneration by puncture (PD) group, containing one post-puncture degenerated disc; Group D is a normal naturally degenerated disc without any intervention (Group ND, nature degenerated group). The first intact coccygeal disc segment was determined to be the standard of normal (ND). The specific construction method is as follows: Using a fluoroscope, a 22G needle was inserted into each rat's caudal coccygeal disc to cause disc degeneration. Two weeks later, needle-damaged caudal segments were transplanted with 50 μL of hBMSCs or hADSCs (1×10^7 cells/mL) by

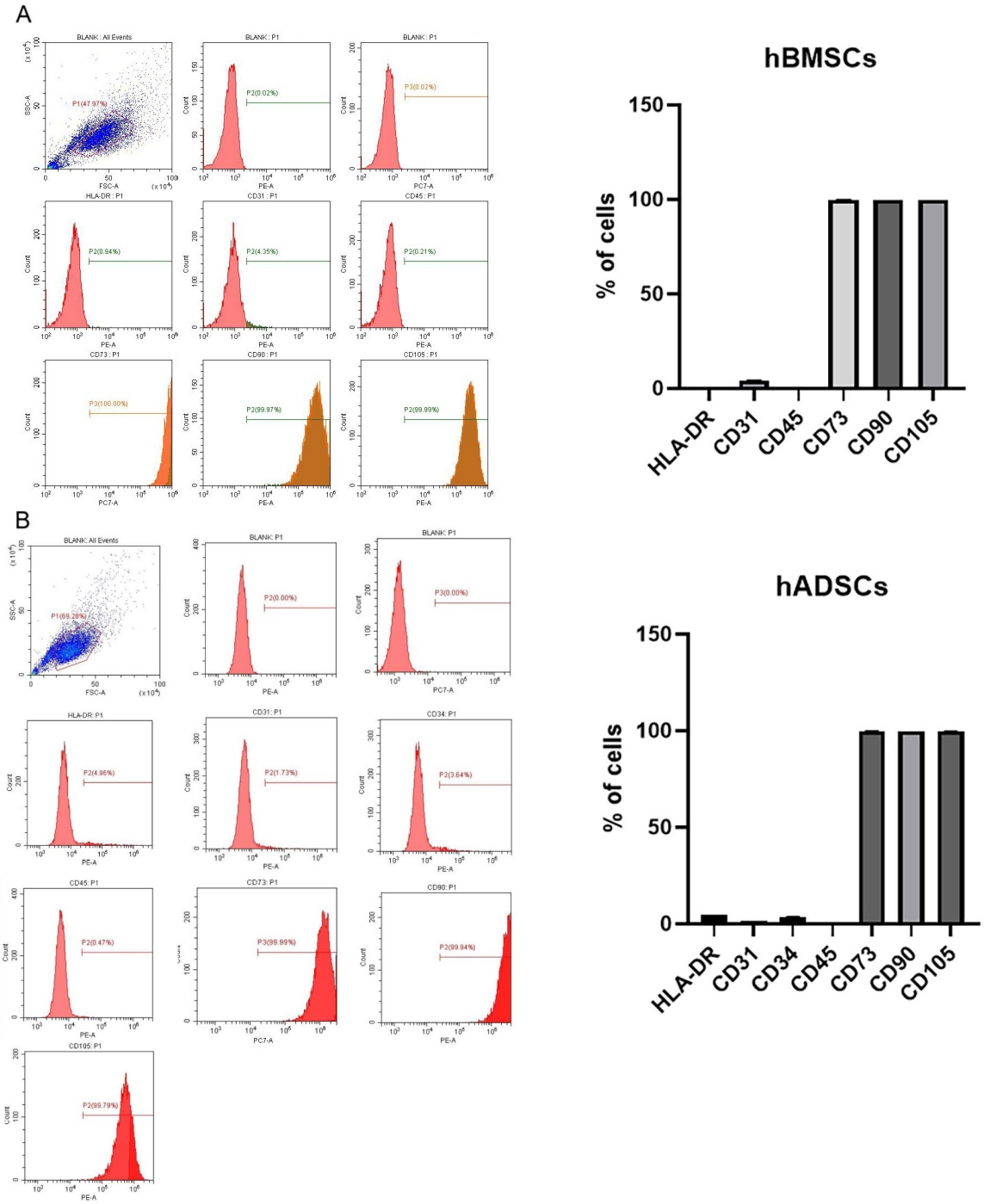

Fig. 2. Detection of hBMSCs and hADSCs surface antigens by flow cytometry. (A) hBMSCs were subjected to flow cytometry to determine the expression of surface antigens, including HLA-DR, CD31, CD45, CD73, CD90, and CD105. (B) hADSCs were subjected to flow cytometry to determine the expression of surface antigens, including HLA-DR, CD31, CD34, CD45, CD73, CD90, and CD105.

injection using a stereotactic micro-injector and a 30G needle syringe; the cells were transplanted at a rate of 10 µL per minute. Instead of hBMSCs or hADSCs, saline was injected into the injured (PD) segment of the other damaged caudal segment.

Radiological Assessment

Magnetic resonance imaging (MRI; 3.0 T Bruker Biospin imager) of tail discs 2, 4, and 6 months following transplantation was performed to assess the efficacy of hBMSCs or hADSCs using the following parameter settings: spin-echo repetition period = 500–4000 seconds;

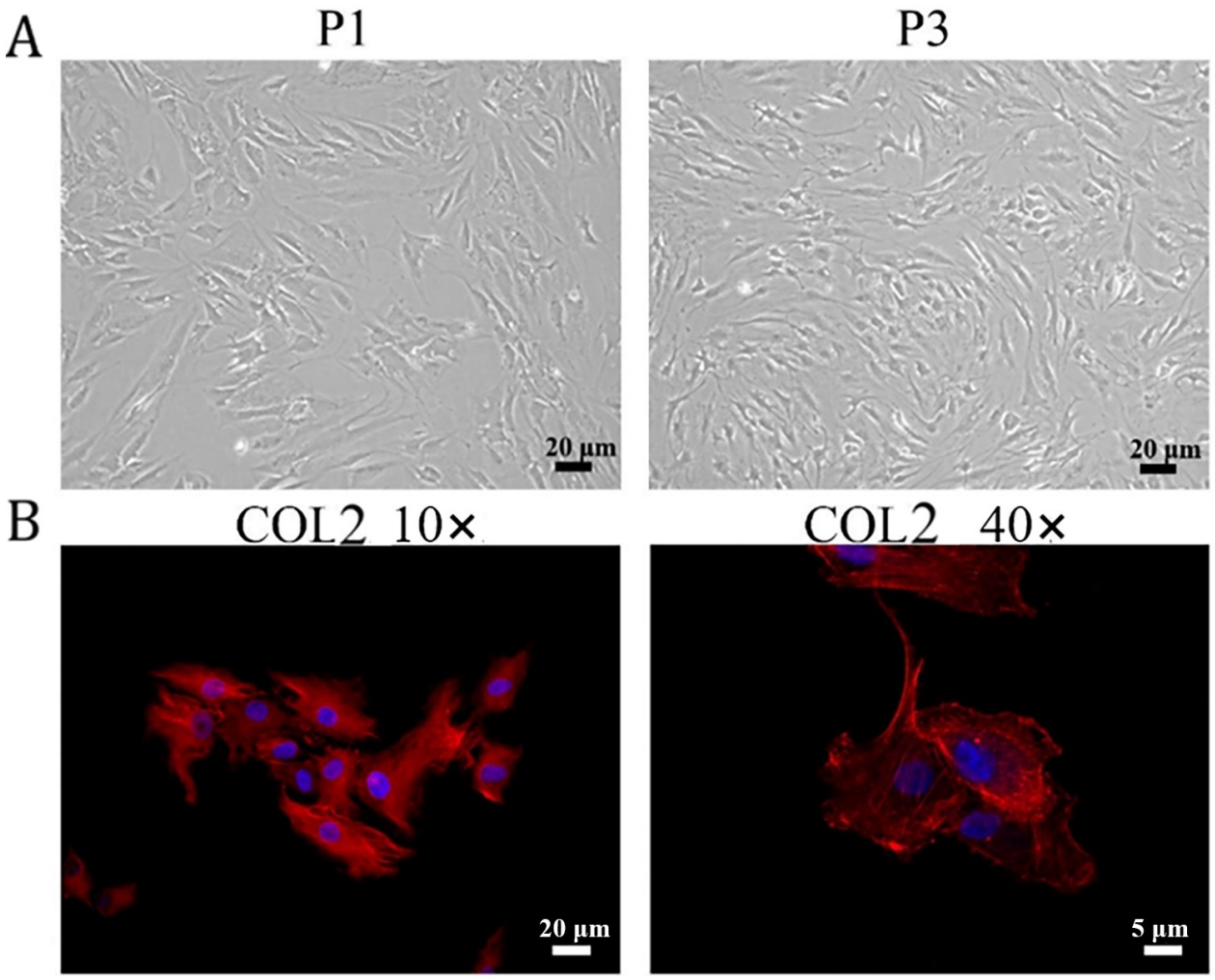

Fig. 3. Morphology and expression of COL2 in human nucleus pulposus cells (hNPCs). (A) Morphology of hNPCs, observed under 10× magnification. P1, first generation; P3, third generation. (B) The immunofluorescence assay was performed to visualize the expression of COL2 of hNPCs, which were viewed under 10× and 40× magnification.

echo duration = 65–123 seconds; 8 excitations, field of view = 12 cm; slice thickness = 2 mm; and phase wrap not used. The disc damage was graded using Paravision software (version 3.0.2; Bruker Biospin AG, Karlsruhe, Germany). All MRI images were independently reviewed by two radiologists and scored according to the Thompson grading scale (Table 1), and the scores of each disc at different times were recorded. The so-called "black disc" effect at T2 weighted image (T2WI) was generally seen in the calibrated degenerated discs, and a Thompson grading of 2 or above was considered for modeling (Table 1).

Histological Assessment

Rats were put to sleep via inhalation anesthesia (i.e., administration of anesthetic gases, such as isoflurane and sevoflurane for use in mice, through a mask or nose cone) before 250 mL of ice-cold 4% paraformaldehyde was transcardially infused into their hearts, followed by administration of 125 mL of normal saline (with 10 U of heparin sodium per 1 mL). Coccygeal vertebrae were removed and then fixed for 48 hours in a 10% formalin solution. Afterward, they were decalcified for three days in 5% nitric acid, which was changed every 24 hours, and then rinsed in an ammonia solution for 30 minutes to neutralize any remaining acid. The acquired vertebral samples were then immersed in paraffin wax and the tissue block was cut into 4 μm slices by microtoming longitudinally. Safranin O (Solarbio Technology, Beijing, China) was used to stain the sections. Disc degeneration was histologically assessed according to the standards set out by Nishimura and Mochida [15] (Table 2).

Immunofluorescence Staining of Rat Intervertebral Disc

After obtaining intervertebral disc sections from rats with the corresponding treatment, the sections were baked in an oven set at 60 °C for 60 minutes for dewaxing and

hydration; placed in a 90 °C water bath for 10 minutes for antigen retrieval and then left to cool; and placed at room temperature and washed thrice with PBS for 3 minutes each time. The sections were blocked using 1% bovine serum albumin (BSA) solution at room temperature for 30 minutes, and the BSA solution was then gently shaken off. An immunohistochemical pen was used to draw a circle around the tissue. Pre-configured primary antibody (type II collagen or SOX9; 1:100 dilution) was added and incubated overnight in the refrigerator at 4 °C. The sections were then washed with PBS thrice for 3 minutes each time. After wiping off the PBS around the tissue, an immunohistochemical pen was used to draw a circle around the tissue. Pre-configured fluorescent secondary antibody was added and incubated in a wet box at room temperature for 60 minutes (protected from light). The sections were washed thrice with PBS for 3 minutes each time. The PBS around the tissues was wiped off. 4′,6-diamidino-2-phenylindole (DAPI, diluted 10 times) was added and incubated for 3 minutes (no more than 5 minutes) at room temperature and shielded from light; the sections were then sealed and observed under the microscope. The immunohistochemical images were captured and the staining results were analyzed quantitatively using ImageJ software (version 1.5.1j8, NIH, National Institutes of Health, Madison, WI, USA).

Induction of Adipogenic Differentiation of hBMSCs or hADSCs

Isolated hBMSCs or hADSCs were cultured in a mixture of Ham's F-12 medium and Dulbecco's Modified Eagle Medium with 10% FBS (control medium) in equivalent proportions. At a seeding density of 400 cells/mm^2, the hADSCs were stimulated in an adipogenic induction medium comprising 200 µM indomethacin, 10 µM insulin, 0.5 µM 3-isobutyl-1-methylxanthine, and 1 µM dexamethasone. The cells were cultured for up to 3 days with media changes every 3 days. After 3 weeks, the cultures were preserved in 10% formalin, and Oil red O staining was performed to measure the degree of adipogenic differentiation.

Induction of Osteogenic Differentiation of hBMSCs or hADSCs

At a seeding density of 200 cells/mm^2, hBMSCs or hADSCs were stimulated in an osteogenic induction medium containing 100 nM dexamethasone, 10 µM b-glycerophosphate, and 5 mg/mL ascorbate-2-phosphate (Sigma). For up to 3 weeks, the cultures were fed with the osteogenic medium every 3 days. The cells were preserved in 10% formalin after 3 weeks, and Alizarin red staining was performed to assess osteogenic differentiation.

Quantitative Real-Time Polymerase Chain Reaction

Trizol reagent (Life Technologies, 15596-026, Carlsbad, CA, USA) was used to isolate total RNA from the specified cells. HiScript III 1st Strand cDNA Synthesis Kit (Vazyme, R312-01, Nanjing, China) was used to synthesize cDNA, and One-Step SYBR® PrimeScript®PLUS RT-RNA PCR Kit (RR057B, Takara, Kyoto, Japan) was used to detect the relative expression levels of the relevant genes. The relative gene expression levels were determined using the $2^{-\Delta\Delta Ct}$ method, and glyceraldehyde 3-phosphate dehydrogenase (*GAPDH*) was used as the internal control. A list of primer sequences is given in Table 3.

Table 3. Sequences of primers used in this study.

Gene	Primers (5′ to 3′)
COL2	Forward primer: TGGACGCCATGAAGGTTTTCT Reverse primer: TGGGAGCCAGATTGTCATCTC
SOX9	Forward primer: AGCGAACGCACATCAAGAC Reverse primer: CTGTAGGCGATCTGTTGGGG
COL4	Forward primer: CATAACCGCTGTGCGGAAAAT Reverse primer: TCATCTAGGGACTTACCACCTG
ACAN	Forward primer: CCCCTGCTATTTCATCGACCC Reverse primer: GACACACGGCTCCACTTGAT
VCAN	Forward primer: GTAACCCATGCGCTACATAAAGT Reverse primer: GGCAAAGTAGGCATCGTTGAAA
KRT19	Forward primer: AACGGCGAGCTAGAGGTGA Reverse primer: GGATGGTCGTGTAGTAGTGGC
HIF1	Forward primer: GAACGTCGAAAAGAAAAGTCTCG Reverse primer: CCTTATCAAGATGCGAACTCACA
CA12	Forward primer: AGTGACATCCTCCAGTATGACG Reverse primer: GTGGCACTGTAGCGAGACT

COL2, type II collagen; *SOX9*, SRY-Box Transcription Factor 9; *COL4*, type IV collagen; *ACAN*, aggrecan; *VCAN*, versican; *KRT19*, cytokeratin 19; *HIF1*, hypoxia-inducible factor 1; *CA12*, carbonic anhydrase 12.

Western Blotting

RIPA lysis buffer (Beyotime, Shanghai, China) was used to extract total protein for use in Western blotting, and the concentration was determined using a Pierce™ BCA Protein Assay Equipment (ThermoFisher, Waltham, MA, USA). Proteins were then isolated using 10% sodium dodecyl sulfate-polyacrylamide gel electrophoresis (SDS-PAGE) and transferred onto polyvinylidene difluoride (PVDF) membranes. The membranes were blocked with nonfat milk and then incubated with anti-rabbit antibodies against type II collagen (COL2), SOX9, type IV collagen (COL4), aggrecan (ACAN), and versican (VCAN) (1:1000 dilution; Ab39670, Abcam, Cambridge, UK), or glyceraldehyde 3-phosphate dehydrogenase (GAPDH) (1:5000 dilution; Ab8245, Abcam, Cambridge, UK) overnight at 4 °C. Antibodies against carbonic anhydrase 12 (CA12; 1:10,000 dilution; Ab195233, Abcam, Cambridge, UK), cytokeratin 19 (KRT19; 1–2 µg/mL dilution; Ab220193, Cambridge, UK), and hypoxia-inducible factor 1 (HIF1;

5 µg/mL dilution; Ab1, Abcam, Cambridge, UK) were also used. We used horseradish peroxidase (HRP) goat anti-rabbit IgG (H+L) (A0208; Beyotime, China) and HRP goat anti-mouse IgG (H+L) (A0216; Beyotime, Shanghai, China) as secondary antibodies. The blots were then viewed using ThermoFisher's enhanced chemiluminescence solution, and Image LabTM Software 5.2 was used to evaluate the signals (BioRad, Hercules, CA, USA).

Immunofluorescence Analysis

Immunofluorescence was applied to examine the differentiation of hBMSCs and hADSCs, as previously reported [16]. Briefly, while the cell density reaches 50% confluency, a solution of 0.5% Triton X-10 was applied to these cells for 5 minutes and then incubated with 200 µL TRITC F-actin for 30 minutes in the dark. Next, DAPI was used to stain the cell nuclei for about 30 seconds. Finally, the cells were observed with a fluorescence microscope. Similarly, COL2 (1:100 dilution; Ab34712, Abcam, Cambridge, UK) and ACAN (1:100 dilution; Ab3773, Abcam, Cambridge, UK) antibodies were applied in the detection of cell differentiation using immunofluorescence.

Statistical Analysis

Statistical analysis was performed using SPSS 24.0 software (IBM Corp., Armonk, NY, USA), and data from at least three experiments were expressed as mean ± standard error (SE). Using the Student's *t*-test, the differences between the hBMSCs and hADSCs groups were calculated. One-way analysis of variance (ANOVA) was used to compare data of 3 or more groups. *p*-value of less than 0.05 denotes that the difference is statistically significant.

Results

Identification and Differentiation Capacity Assessment of hBMSCs and hADSCs

The primary hBMSCs and hADSCs obtained from the patients were morphologically heterogeneous, displaying a mixture of spindle-shaped, large flat cells , or tiny spherical cells. The tiny spherical cells rapidly vanished during the course of the passages and took on a more fibroblast-like form (Fig. 1A). According to earlier research on BMSCs and ADSCs, the fibroblast-like shape predominated in the third passage (Fig. 1B). The viability of these cells was examined by performing CCK-8 assays at the indicated time (day 1, 2, 5, 7, 9). As shown in Fig. 1E, the *in vitro* proliferation of both BMSCs and ADSCs shows the typical S-shaped growth curve. These results indicated the successful isolation of both BMSC and ADSC cells, which presented robust cell growth. Meanwhile, we found that the overall growth rate of hADSCs was slightly faster than that of hBMSCs.

To test the cellular function of the isolated hBMSCs and hADSCs, their ability to differentiate into adipocytes and osteoblasts was evaluated. Dark ECM material was seen under osteogenic induction circumstances following the induction period (Fig. 1C), which was verified by the positive Alizarin red staining. Lipid droplets accumulated in the induced hBMSCs and hADSCs following 21 days of culture in the adipogenic induction media, as verified by the positive Oil red O staining (Fig. 1D). Additionally, flow cytometric analysis revealed that the human MSC markers, such as CD105, CD90, and CD73, were expressed by the hBMSCs and hADSCs with higher than 90% expression level (Fig. 2A,B). Meanwhile, the markers CD45, CD34, and HLA-DR specific for blood cells were all expressed at low levels, which were less than 5%. This suggested that high-activity and high-purity hBMSCs and hADSCs were successfully derived, which were then used for further experiments.

Cultivation and Identification of hNPCs

High-purity cells, which are round, short-spindle, or polygonal, were obtained, as shown in Fig. 3. Subsequently, an immunofluorescence assay was performed to examine the expression of COL2, which is specifically accumulated in NP cells. As shown in Fig. 3, high fluorescence intensity was observed in these cells, suggesting the isolated hNPCs were fully functional and of high purity; the high-purity cells were then used in further assays.

hADSCs and hBMSCs were Induced to Differentiate into hNPCs by Non-Contact Co-Culture with hNPCs

To evaluate the ability of hADSCs and hBMSCs to differentiate into hNPCs, these cells were co-cultured with hNPCs in a non-contact manner. After co-culture for 7 days, the morphology of hBMSCs and hADSCs was observed under a confocal microscope. As shown in Fig. 4A, the uniform long spindle-shaped cells appeared as round and short fusiform with pseudopodia remaining on the edge of the cell, resembling the morphology of hNPCs. This indicates that both hADSCs and hBMSCs can differentiate into NP cells. Additionally, we examined the cellular activity of differentiated hADSCs and hBMSCs by utilizing an immunofluorescence assay to visualize the expression of COL2 and ACAN. We observed that there was a considerable accumulation of both COL2 and ACAN in hADSCs and hBMSCs (Fig. 4B). These results together indicated that both hADSCs and hBMSCs can be effectively induced into NP cells by a co-culture with hNPCs. To further confirm this postulation, we performed qRT-PCR and Western blotting and found that, compared with those cultured alone, the mRNA and protein levels of COL2, SOX9, COL4, ACAN, and VCAN, which are specific markers of NP cells, were all significantly increased in hADSCs or hBMSCs co-cultured with hNPCs (Fig. 5A–C). Meanwhile, the mRNA and protein levels of COL2, SOX9, ACAN, CA12, KRT19, and HIF1 were compared between hADSCs and hBMSCs, as shown in Fig. 5D,E. These markers manifested more pronounced expression in hBMSCs co-cultured

with hNPCs than in the hADSCs counterpart, suggesting that compared to hADSCs, hBMSCs have a stronger ability to differentiate into hNPCs.

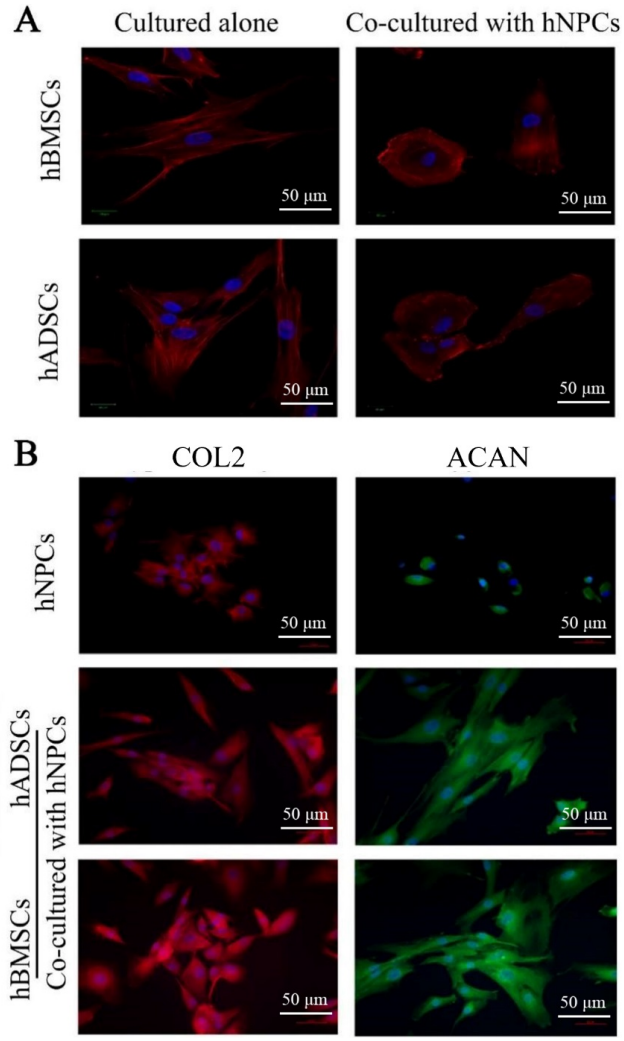

Fig. 4. hBMSCs and hADSCs co-cultured with hNPCs. (A) hBMSCs and hADSCs were non-contact co-cultured with hNPCs for 7 days. After 4′,6-diamidino-2-phenylindole (DAPI) staining, the morphology of hADSCs and hBMSCs was observed under a confocal microscope. (B) The expression of COL2 and ACAN in hBMSCs and hADSCs, regardless of whether they were co-cultured with hNPCs, was observed under a confocal microscope after DAPI staining.

hADSCs and hBMSCs Transplantation Alleviated the IVD in Rats

To determine the IVD treatment effect of hADSCs and hBMSCs, we first established a rat IVD model by puncturing intervertebral discs in the rat's tail. Eight weeks after the puncture, the discs in the rat's tail were examined with MRI, as shown in Fig. 6A. The typical "black disc" effect was noted in the punctured discs but not in the unpunctured ones, indicating the degeneration of intervertebral disc models had taken place. Afterward, hBMSCs and hADSCs were transplanted to the rats with degenerated intervertebral discs, and the untreated rats with punctured degeneration disc (PD) were used as control. Every 2 months after cell transplantation until the 6th month, the intervertebral discs were examined with MRI to determine the treatment effect of hBMSCs and hADSCs. As revealed in Fig. 6B, the degree of IVD gradually improved in the hADSCs, hBMSCs, and PD groups, but not in the naturally degenerated (ND) group. Meanwhile, the progression of IVD in hADSCs and hBMSCs groups was found to be slightly attenuated as compared with the PD groups, although the differences were not statistically significant. Further, histomorphological observations were carried out and scored 6 months after cell transplantation to determine the therapeutic effect of hBMSCs and hADSCs. No significant improvement was observed in the intervertebral discs of the ND group, but the IVD in PD, hADSCs, and hBMSCs groups were improved in varying degrees. As evidenced by the structural destruction of the NP area with almost no NP cells, the peripheral annulus fibrosus was disorderly arranged, ruptured or twisted; the cartilage endplates were incomplete on both the left and right sides, and the cartilage cells were reduced in number, and even replaced by granulation tissue, as shown in Fig. 7A,B. Nevertheless, IVD was less pronounced in the hADSCs and hBMSCs cohorts than in the PD cohort ($p < 0.05$ and $p < 0.01$, respectively), but there was no significant difference between hADSCs- and hBMSCs-treated groups.

Additionally, an immunofluorescence assay was used to gauge the buildup of COL2 and SOX9 proteins in the NP. Both COL2 and SOX9 were substantially expressed in the nucleus pulposus of the ND group, with the COL2 being expressed in the cytoplasm and SOX9 in the nucleus of the NP, as shown in Fig. 8. Additionally, as predicted, the expression of these proteins was significantly lower in the PD, hADSCs, and hBMSCs groups compared to the ND group, with PD group exhibiting the most pronounced reduction in COL2 and SOX9 protein levels. In contrast, there was no significant difference in COL2 and SOX9 accumulation between the hADSCs and hBMSCs groups. This finding suggested that the transplantation of hADSCs or hBMSCs may partially restore the expression of COL2 and SOX9 in the NP and thus lessen the degeneration of the intervertebral disc.

Discussion

Human marrow mesenchymal stem cells (hMSCs) transplantation into the degenerated discs has been shown to increase the water content of the hNPCs, maintain the height of intervertebral space, as well as significantly alleviate the pain in the lower back of patients [17–19]. Although the therapeutic effect of autologous hMSCs in IVD has been

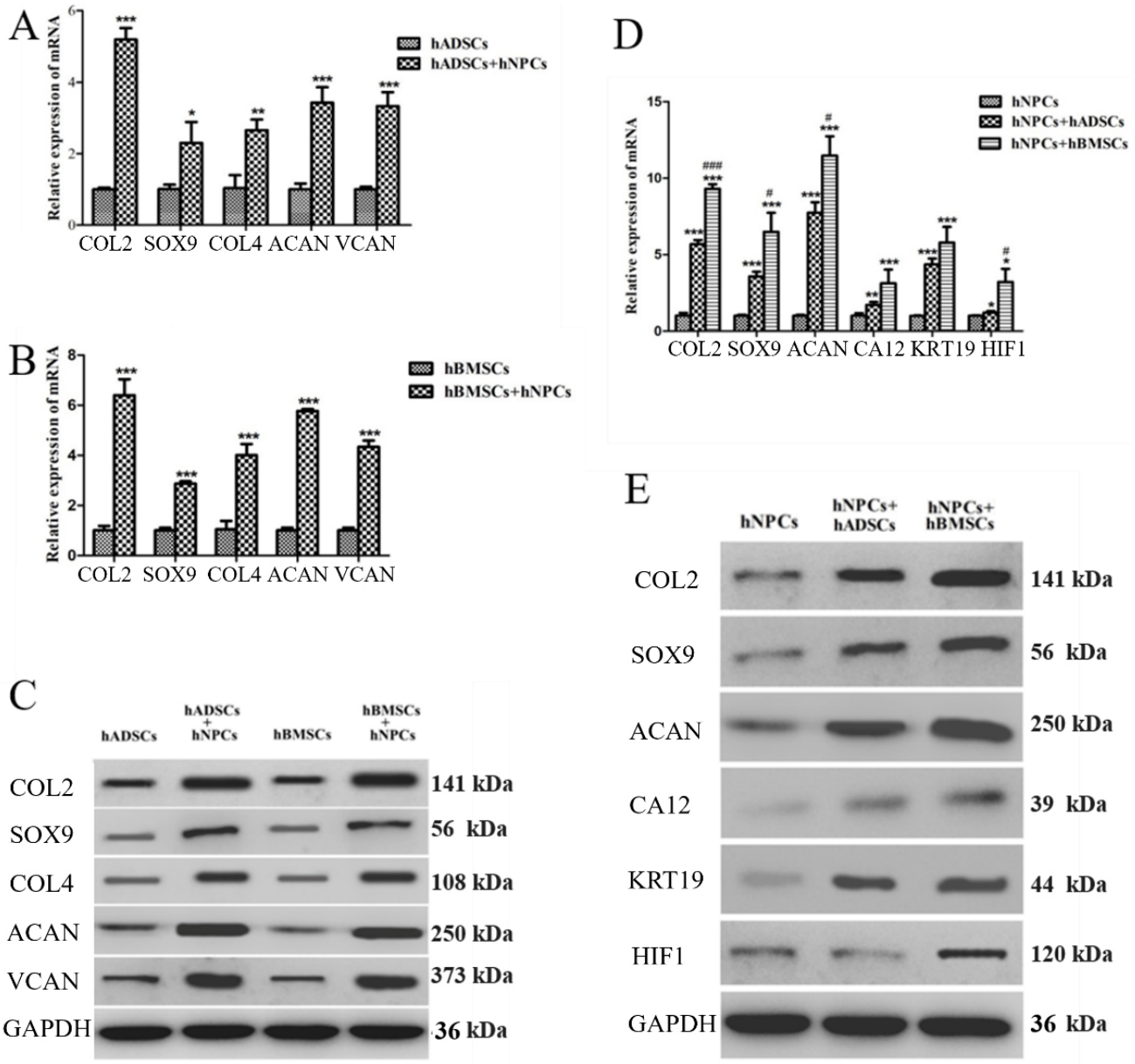

Fig. 5. Expression of hNPCs markers in hADSCs and hBMSCs. (A) The mRNA levels of *COL2*, *SOX9*, *COL4*, *ACAN*, and *VCAN* in hADSCs and hADSCs co-cultured with hNPCs. (B) The mRNA levels of *COL2*, *SOX9*, *COL4*, *ACAN*, and *VCAN* in hBMSCs and hBMSCs co-cultured with hNPCs. (C) The protein levels of COL2, SOX9, COL4, ACAN, and VCAN between hADSCs and hADSCs co-cultured with hNPCs, and between hBMSCs and hBMSCs co-cultured with hNPCs. (D) The mRNA and protein levels of COL2, SOX9, ACAN, CA12, KRT19, and HIF1 were determined in hNPCs alone and hBMSCs and hADSCs that were co-cultured with hNPCs. Notes: $^{*}p < 0.05$, $^{**}p < 0.01$, $^{***}p < 0.001$, compared with hNPCs; $^{\#}p < 0.05$, $^{\#\#\#}p < 0.001$, compared with hNPCs+hADSCs. (E) The protein levels of COL2, SOX9, ACAN, CA12, KRT19, and HIF1 were determined in hNPCs alone and hBMSCs and hADSCs that were co-cultured with hNPCs. n = 3.

proven to be valid [11,20], there are still a few limitations in its application. The effectiveness and safety of hMSCs in the treatment of IVD are evidenced by the improvement rate after treatment of about 60% on average and the absence of serious adverse events, but treatment with hMSCs does not result in an obvious improvement in imaging results, such as MRI, consistent with the results presented in Fig. 6 [21]. Despite the favorable treatment effects, previous studies utilized a very small sample size, rendering the findings not valid enough to support translation into a wider range of clinical applications. Of note, the treatment involving MSCs is very costly, mainly due to the difficulty in obtaining sufficient hMSCs. Besides, the extraction of autologous bone marrow hMSCs is a time-consuming process, and obtaining enough cells with high biological activity can be challenging. In addition, systemic diseases

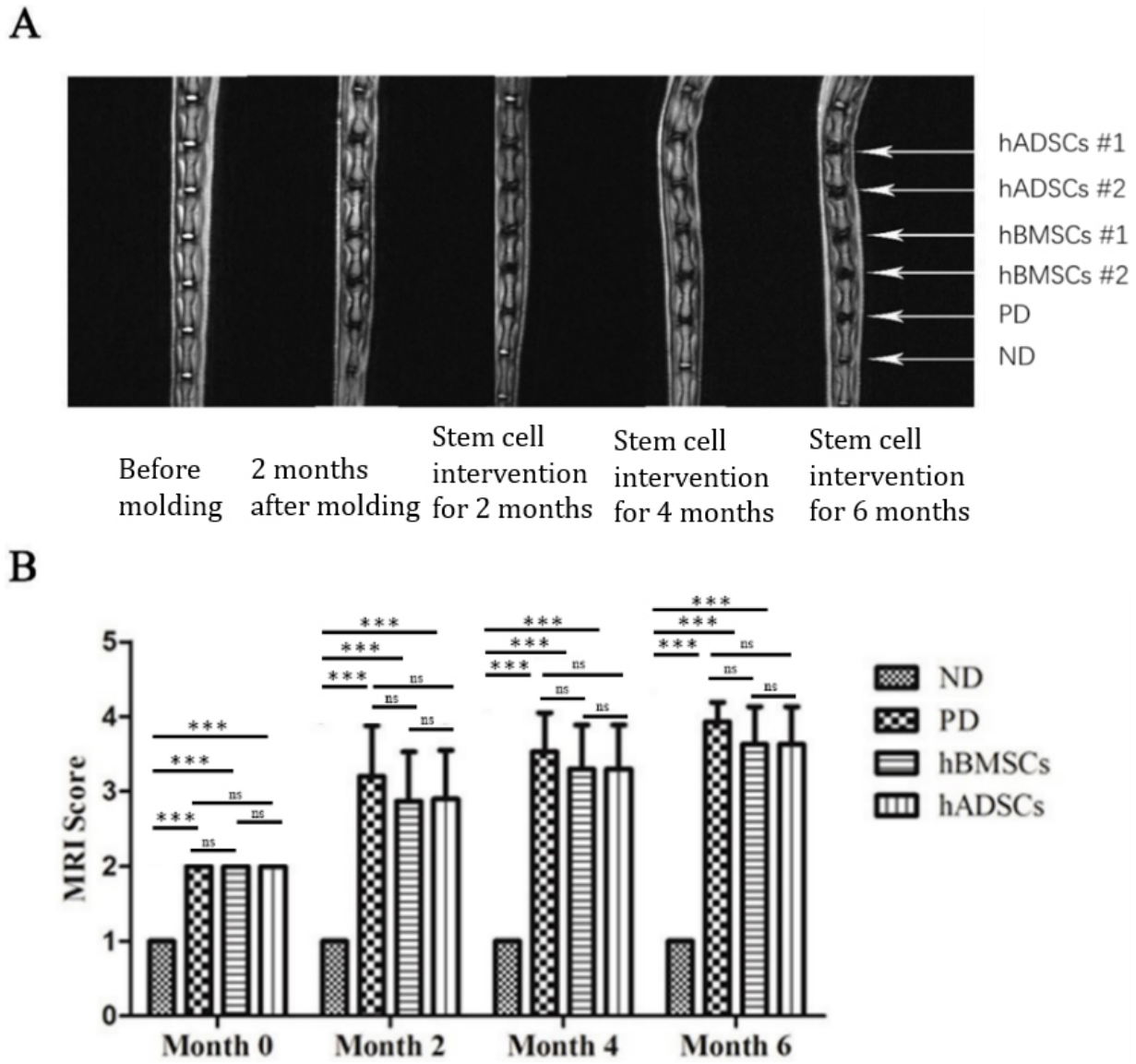

Fig. 6. Magnetic resonance imaging (MRI) detection of the rat tail discs. (A) MRI scan of the rat tail discs before or after stem cell transplantation at the indicated time. (B) MRI score of nature degenerated (ND), degeneration by puncture (PD), hBMSCs and hADSCs groups. ns, $p > 0.05$; ***$p < 0.001$, compared with ND group; n = 15.

in donors can alter the intrinsic characteristics of hMSCs [19]. Nevertheless, the low immunogenicity and immunosuppressive properties of MSCs obviate the need for immunosuppression in the recipients.

However, it is currently unclear whether hADSCs have similar properties to hBMSCs when it comes to allogeneic transplantation. Most previous studies on IVD therapy have focused on hBMSCs, with limited studies on hADSCs. However, it has been demonstrated that hADSCs possess a multipotent mesenchymal differentiation capacity comparable to that of hBMSCs [22]. In the meantime, hADSCs can be collected through minimally invasive and straightforward surgical techniques, which are commonly used in obesity treatment. Thus, it is easier to obtain a larger quantity of hADSCs compared to hBMSCs. Furthermore, under normal tissue culture conditions, hADSCs can easily survive and be separated into their component cells using random enzyme-based separation techniques [23]. Given these advantages, it is important to conduct further research to determine the therapeutic effects of hADSCs on IVD. Therefore, the potential of hADSCs to treat IVD was explored in this study.

When exposed to the right stimuli, hMSCs may develop into osteoblasts, chondroblasts, adipocytes, or hepatocytes. The fundamental elements of the intervertebral disc, such as COL2, ACAN and anionic proteoglycans, are produced by hMSCs when they differentiate into NP cells [24]. There is no significant difference between hADSCs and hBMSCs concerning their immunogenicity and capacity to differentiate into specialized cells [22]. Additionally,

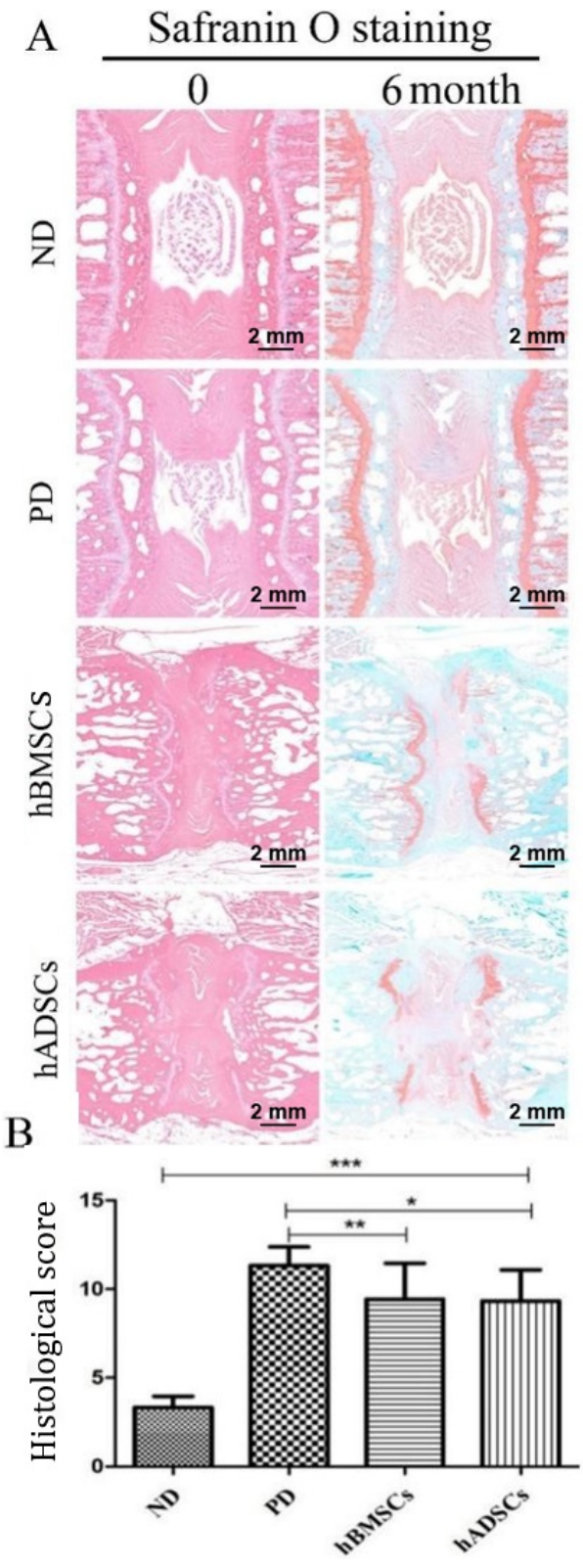

Fig. 7. Histomorphological observation of rat tail discs. (A) Six months after cell transplantation, Safranin O staining was conducted to stain degenerated intervertebral discs, cartilage endplates, and nuclei pulposus; n = 15. (B) The corresponding tissue alteration was scored. *$p < 0.05$, **$p < 0.01$, ***$p < 0.001$.

a large number of hADSCs can be easily obtained for clinical application by performing liposuction, which is commonly used for cosmetic reasons [22]. Thus, hADSCs represent a more attractive option over hBMSC. In the present study, both human hBMSCs and hADSCs were successfully isolated. Further, both BMSCs and hADSCs were found to be induced into hNPCs as the differentiated hBMSCs and hADSCs exhibited NPCs-like form and the marker genes specific for hNPCs were strongly expressed in these cells. Furthermore, both hBMSCs and hADSCs were found to effectively attenuate the degeneration of the intervertebral disc, as revealed by MRI and histological assays. More importantly, the therapeutic efficacy of hBMSCs and hADSCs on IVD was not significantly different, suggesting that hADSCs are as potent as hBMSCs in the treatment of IVD.

There are some controversies regarding the mechanism underlying the attenuation of disc degeneration and the restoration of disc function by the transplanted hMSCs. As demonstrated in some studies, in response to the requirements of injured host tissues, hMSCs have been shown to differentiate into hNP cells and produce a range of cytokines and growth factors that promote host tissue regeneration, and thus promote the restoration of the degenerated discs [25,26]. Several studies also reported that the synthesis of the ECM and the subsequent water restoration within discs after hMSCs transplantation restored the function of the intervertebral disc [27–29]. We postulate that both above-mentioned mechanisms contributed to the prolonged therapeutic effect of hBMSCs and hADSCs, as the current study found that both hBMSCs and hADSCs can be induced into hNPCs and can effectively express COL2, which is specifically expressed in hNPCs when these cells were co-cultured with hNPCs. The main limitation of this study is that the stem cells were obtained from only one human donor. It would be helpful if more human donors could participate in future studies.

In the present study, hNPCs were non-contact co-cultured with hBMSCs and hADSCs to examine their capacity to develop into NPCs. It was revealed that both hBMSCs and hADSCs could effectively differentiate into hNPCs after being co-cultured with hNPCs, but hADSCs showed a lower efficacy in this regard relative to hBMSCs. Further, hBMSCs and hADSCs were separately injected into the degenerated intervertebral discs of rats to compare their therapeutic effects on IVD. The results showed that the NP expressing COL2 and SOX9 proteins was dramatically increased in both hBMSCs and hADSCs groups compared to the control group, and IVD was shown to be attenuated in both hBMSCs and hADSCs groups. Moreover, there was no significant difference between hBMSCs and hADSCs groups regarding their treatment effect on IVD. Collectively, our findings provide a key experimental framework for using MSCs in the treatment of IVD.

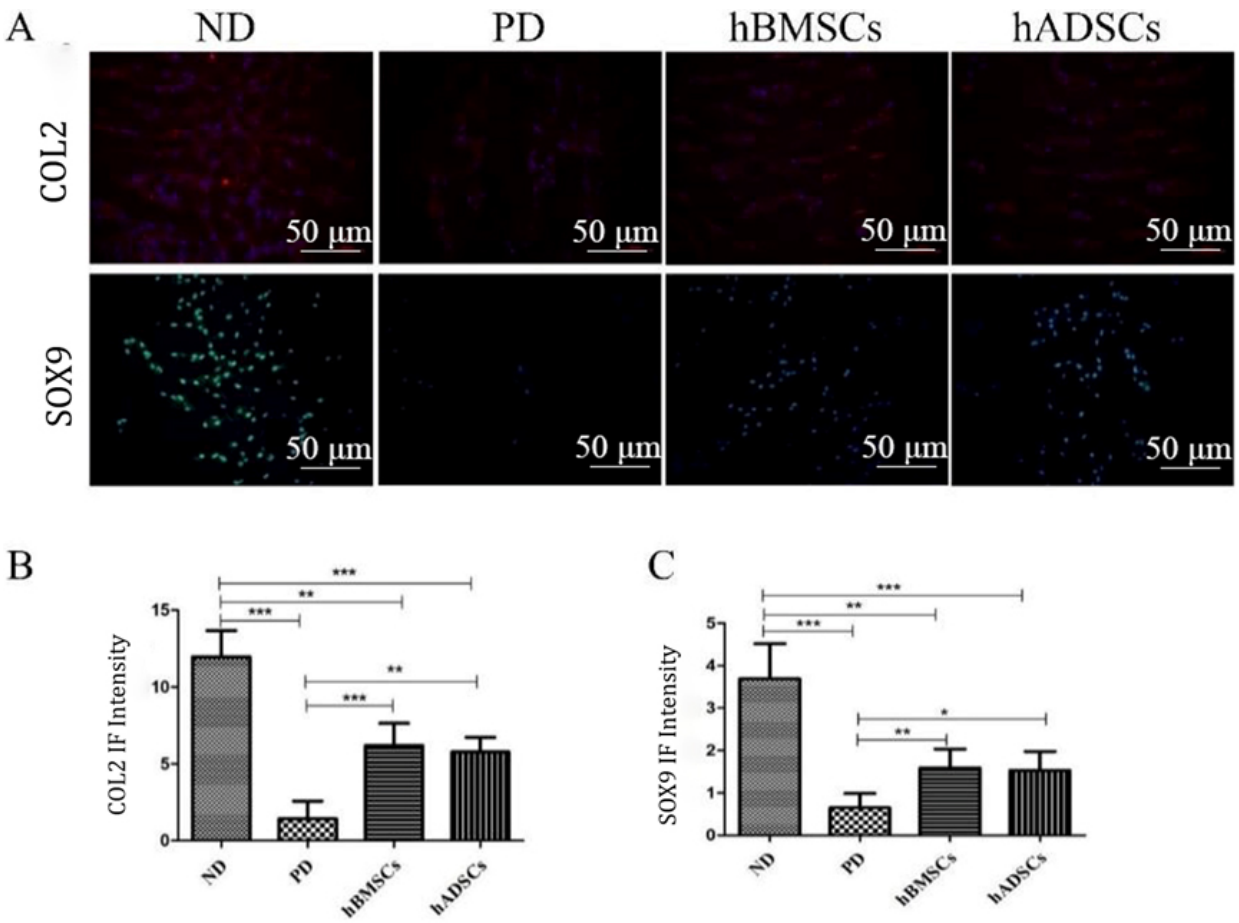

Fig. 8. Detection of COL2 and SOX9 in the nucleus pulposus. (A) The immunofluorescence test was performed to detect COL2 and SOX9 accumulation in the nucleus pulposus of ND, PD, and hBMSCs or hADSCs groups; n = 15. (B) Statistic result of COL2 IF intensity. (C) Statistic result of SOX9 IF intensity. $*p < 0.05$, $**p < 0.01$, $***p < 0.001$.

Conclusions

In summary, both hADSCs and hBMSCs can attenuate and delay the progression of IVD, but not completely reverse the pathological process, and there is no significant difference between hADSCs and hBMSCs in terms of their therapeutic effects on IVD. Given their extraordinary performance in allogeneic xenotransplantation, hADSCs and hBMSCs can serve as ideal therapeutic agents in IVD treatment.

Availability of Data and Materials

Upon request, the corresponding author will provide the data supporting the findings of this study.

Author Contributions

JZ, JP, GD, XL and ZZ: Conceptualization, Methodology, Software, Investigation, Formal Analysis, Writing — Original Draft. LL and BS: Conceptualization, Funding Acquisition, Resources, Supervision, Writing — Review & Editing. All the authors have been involved in drafting the manuscript or revising and all the authors have given final approval for the version to be published. Each author has participated sufficiently in the work to take public responsibility for appropriate portions of the content. All the authors have agreed to be accountable for all aspects of the work in ensuring that questions related to the accuracy or integrity of any part of the work are appropriately investigated and resolved.

Ethics Approval and Consent to Participate

Shanghai East Hospital (East Hospital Affiliated to Tongji University) Medical Ethics Committee approved the study protocol, which met the relevant guidelines and regulations of Shanghai Medical Ethics Committee. The human ethics statement number is [2017] YSD No. 098. The animal ethics statement number is [2017] Animal Experimental Ethical Inspection No. 149. The research is performed in accordance with the Declaration of Helsinki. All included volunteers had signed an informed consent form.

Acknowledgment

Not applicable.

Funding

The research was supported by Shanghai Municipal Health Commission (Grant Number: 201940283) and Science and Technology Plan of Jiangxi Health Commission (Grant Number: SKJP220218218).

Conflict of Interest

The authors declare no conflict of interest.

References

[1] Li G, Zhang W, Liang H, Yang C. Epigenetic regulation in intervertebral disc degeneration. Trends in Molecular Medicine. 2022; 28: 803–805.

[2] Fernandez-Moure J, Moore CA, Kim K, Karim A, Smith K, Barbosa Z, *et al*. Novel therapeutic strategies for degenerative disc disease: Review of cell biology and intervertebral disc cell therapy. SAGE Open Medicine. 2018; 6: 2050312118761674.

[3] Zhang F, Zhao X, Shen H, Zhang C. Molecular mechanisms of cell death in intervertebral disc degeneration (Review). International Journal of Molecular Medicine. 2016; 37: 1439–1448.

[4] Kepler CK, Ponnappan RK, Tannoury CA, Risbud MV, Anderson DG. The molecular basis of intervertebral disc degeneration. The Spine Journal: Official Journal of the North American Spine Society. 2013; 13: 318–330.

[5] Ding F, Shao ZW, Xiong LM. Cell death in intervertebral disc degeneration. Apoptosis: an International Journal on Programmed Cell Death. 2013; 18: 777–785.

[6] Matta A, Karim MZ, Gerami H, Jun P, Funabashi M, Kawchuk G, *et al*. NTG-101: A Novel Molecular Therapy that Halts the Progression of Degenerative Disc Disease. Scientific Reports. 2018; 8: 16809.

[7] Leckie SK, Bechara BP, Hartman RA, Sowa GA, Woods BI, Coelho JP, *et al*. Injection of AAV2-BMP2 and AAV2-TIMP1 into the nucleus pulposus slows the course of intervertebral disc degeneration in an in vivo rabbit model. The Spine Journal: Official Journal of the North American Spine Society. 2012; 12: 7–20.

[8] Yue B, Lin Y, Ma X, Xiang H, Qiu C, Zhang J, *et al*. Survivin-TGFB3-TIMP1 Gene Therapy Via Lentivirus Vector Slows the Course of Intervertebral Disc Degeneration in an In Vivo Rabbit Model. Spine. 2016; 41: 926–934.

[9] Croft AS, Illien-Jünger S, Grad S, Guerrero J, Wangler S, Gantenbein B. The Application of Mesenchymal Stromal Cells and Their Homing Capabilities to Regenerate the Intervertebral Disc. International Journal of Molecular Sciences. 2021; 22: 3519.

[10] Hajiesmailpoor A, Mohamadi O, Farzanegan G, Emami P, Ghorbani M. Overview of Stem Cell Therapy in Intervertebral Disc Disease: Clinical Perspective. Current Stem Cell Research & Therapy. 2023; 18: 595–607.

[11] Liao Z, Li S, Lu S, Liu H, Li G, Ma L, *et al*. Metformin facilitates mesenchymal stem cell-derived extracellular nanovesicles release and optimizes therapeutic efficacy in intervertebral disc degeneration. Biomaterials. 2021; 274: 120850.

[12] Ding N, Li E, Ouyang X, Guo J, Wei B. The Therapeutic Potential of Bone Marrow Mesenchymal Stem Cells for Articular Cartilage Regeneration in Osteoarthritis. Current Stem Cell Research & Therapy. 2021; 16: 840–847.

[13] Ouyang A, Cerchiari AE, Tang X, Liebenberg E, Alliston T, Gartner ZJ, *et al*. Effects of cell type and configuration on anabolic and catabolic activity in 3D co-culture of mesenchymal stem cells and nucleus pulposus cells. Journal of Orthopaedic Research: Official Publication of the Orthopaedic Research Society. 2017; 35: 61–73.

[14] Zhang J, Li Z, Chen F, Liu H, Wang H, Li X, *et al*. TGF-β1 suppresses CCL3/4 expression through the ERK signaling pathway and inhibits intervertebral disc degeneration and inflammation-related pain in a rat model. Experimental & Molecular Medicine. 2017; 49: e379.

[15] Jeong JH, Jin ES, Min JK, Jeon SR, Park CS, Kim HS, *et al*. Human mesenchymal stem cells implantation into the degenerated coccygeal disc of the rat. Cytotechnology. 2009; 59: 55–64.

[16] Li S, Guan H, Zhang Y, Li S, Li K, Hu S, *et al*. Bone marrow mesenchymal stem cells promote remyelination in spinal cord by driving oligodendrocyte progenitor cell differentiation via TNFα/RelB-Hes1 pathway: a rat model study of 2,5-hexanedione-induced neurotoxicity. Stem Cell Research & Therapy. 2021; 12: 436.

[17] Alini M, Diwan AD, Erwin WM, Little CB, Melrose J. An update on animal models of intervertebral disc degeneration and low back pain: Exploring the potential of artificial intelligence to improve research analysis and development of prospective therapeutics. JOR Spine. 2023; 6: e1230.

[18] Armitage AJ, Miller JM, Sparks TH, Georgiou AE, Reid J. Efficacy of autologous mesenchymal stromal cell treatment for chronic degenerative musculoskeletal conditions in dogs: A retrospective study. Frontiers in Veterinary Science. 2023; 9: 1014687.

[19] Sanghani-Kerai A, Black C, Cheng SO, Collins L, Schneider N, Blunn G, *et al*. Clinical outcomes following intra-articular injection of autologous adipose-derived mesenchymal stem cells for the treatment of osteoarthritis in dogs characterized by weight-bearing asymmetry. Bone & Joint Research. 2021; 10: 650–658.

[20] Brennan MÁ, Layrolle P, Mooney DJ. Biomaterials functionalized with MSC secreted extracellular vesicles and soluble factors for tissue regeneration. Advanced Functional Materials. 2020; 30: 1909125.

[21] Sakai D, Andersson GBJ. Stem cell therapy for intervertebral disc regeneration: obstacles and solutions. Nature Reviews. Rheumatology. 2015; 11: 243–256.

[22] Zhu Y, Liu T, Song K, Fan X, Ma X, Cui Z. Adipose-derived stem cell: a better stem cell than BMSC. Cell Biochemistry and Function. 2008; 26: 664–675.

[23] Szabłowska-Gadomska I, Humięcka M, Brzezicka J, Chróścicka A, Płaczkowska J, Ołdak T, *et al*. Microbiological Aspects of Pharmaceutical Manufacturing of Adipose-Derived Stem Cell-Based Medicinal Products. Cells. 2023; 12: 680.

[24] Pattappa G, Li Z, Peroglio M, Wismer N, Alini M, Grad S. Diversity of intervertebral disc cells: phenotype and function. Journal of Anatomy. 2012; 221: 480–496.

[25] Chopp M, Li Y. Treatment of neural injury with marrow stromal cells. The Lancet. Neurology. 2002; 1: 92–100.

[26] Jendelová P, Herynek V, Urdzíková L, Glogarová K, Kroupová J, Andersson B, *et al*. Magnetic resonance tracking of transplanted bone marrow and embryonic stem cells labeled by iron oxide nanoparticles in rat brain and spinal cord. Journal of Neuroscience Research. 2004; 76: 232–243.

[27] Le Visage C, Kim SW, Tateno K, Sieber AN, Kostuik JP, Leong KW. Interaction of human mesenchymal stem cells with disc cells: changes in extracellular matrix biosynthesis. Spine. 2006; 31: 2036–2042.

[28] Sakai D, Mochida J, Iwashina T, Hiyama A, Omi H, Imai M, *et al*. Regenerative effects of transplanting mesenchymal stem cells embedded in atelocollagen to the degenerated intervertebral disc. Biomaterials. 2006; 27: 335–345.

[29] Li L, Sheng K, Mannarino M, Jarzem P, Cherif H, Haglund L. o-Vanillin Modulates Cell Phenotype and Extracellular Vesicles of Human Mesenchymal Stem Cells and Intervertebral Disc Cells. Cells. 2022; 11: 3589.